SPARSE RECONSTRUCTION FOR FLUORESCENCE LIFETIME IMAGING MICROSCOPY WITH POISSON NOISE

Lasith Adhikari, Arnold D. Kim, and Roummel F. Marcia

Applied Mathematics, University of California, Merced, Merced, CA 95343, USA

ABSTRACT

We present a novel, three-stage method to solve the fluorescence lifetime imaging problem under low-photon conditions. In particular, we reconstruct the fluorophore concentration along with its support and fluorescence lifetime from the time-dependent measurements of scattered light exiting the domain. Because detectors used for these problems are photon counting devices, measurements are corrupted by Poisson noise. Consequently, we explicitly consider Poisson noise in conjunction with SPIRAL-ℓ_p – a sparsity-promoting nonconvex optimization method – to solve this problem. We demonstrate the effectiveness of the proposed three-stage method through numerical experiments in 2D fluorescence lifetime imaging.

***Index Terms*—** Fluorescence lifetime imaging (FLIM), photon-limited imaging, Poisson noise, sparse reconstruction, SPIRAL-ℓ_p

1. INTRODUCTION

Fluorescence microscopy provides the ability to study *in vivo* cellular and molecular dynamics in real time, because of its sensitivity, specificity, and versatility [1]. In particular, fluorescence lifetime imaging (FLIM) is becoming increasingly important. The lifetime of a fluorophore provides useful information about the local environment (pH, ion, or oxygen concentration), but not on the local fluorophore concentration or absorption in the sample, etc [1, 2].

In fluorescence lifetime imaging, one seeks to reconstruct the spatial distribution of the fluorescence decay rates within the tissue sample. Typically, this spatial distribution is sparse. Consequently, there have been several recent studies that employed sparsity-promoting methods to solve this FLIM problem. However, these methods minimize the least-squares cost functional with Gaussian noise, *e.g.* [3, 4]. Implicitly, these studies assume that there is enough signal in the measurements made by photon counting detectors that Gaussian noise is a valid assumption. In contrast, we consider here time-dependent measurements with relatively low photon counts. For that case, we must consider measurements corrupted by Poisson noise [5]. To do so, we use the nonconvex Sparse Poisson Intensity Reconstruction ALgorithm (SPIRAL-ℓ_p) [6] to minimize the ℓ_p-norm penalized negative Poisson log-likelihood function. We show that this approach applied to the time-averaged data provides an effective method for reconstructing the spatial support of the fluorophores. Upon determining these supports, we recover the fluorescence decay rates from the time-dependent data. Using numerical simulations, we show that this reconstruction method effectively solves this time-dependent FLIM problem.

This work was supported by National Science Foundation Grant CMMI-1333326. Lasith Adhikari's research is supported by the UC Merced Graduate Student Opportunity Fellowship Program.

2. PROBLEM FORMULATION

For the fluorescence-lifetime imaging problem, we seek to reconstruct the fluorophore concentration along with the support and fluorescence-lifetime from the time-dependent measurements of emitted light due to pulsed excitation of a strongly scattering medium. We assume that the optical properties of the medium are known to reasonable precision. In what follows, we describe the forward model and then the corresponding inverse problem for this fluorescence-lifetime imaging problem.

Forward model: Let Ω denote the domain with boundary $\partial\Omega$. A pulse of exciting light is injected into Ω on $\partial\Omega$. Let $S(\mathbf{r}, t)$ for $\mathbf{r} \in \partial\Omega$ and $t > 0$ denote that exterior time-dependent source of exciting light. Let $I^e(\mathbf{r}, t)$ denotes the intensity of this exciting light source at position $\mathbf{r} \in \Omega$ at time $t \in [0, T]$. It is governed by the following initial-boundary value problem for the diffusion approximation [7, 8]:

$$\frac{1}{c}\frac{\partial I^e}{\partial t} - \nabla \cdot (\kappa^e \nabla I^e) + \mu_a^e I^e = 0 \quad \text{in } \Omega \times (0, T], \tag{1}$$

with κ^e denoting the diffusion coefficient and μ_a^e denoting the absorption coefficient at the exciting wavelength. We solve (1) subject to initial condition

$$I^e(\mathbf{r}, 0) = 0 \quad \text{in } \Omega, \tag{2}$$

and boundary condition

$$I^e + \alpha^e \kappa^e \frac{\partial I^e}{\partial n} = \begin{cases} \gamma^e S(\mathbf{r}, t) & \text{on } \mathbf{r} \in \mathbf{r}_s \\ 0 & \text{on } \mathbf{r} \in \partial\Omega \backslash \mathbf{r}_s \end{cases} \tag{3}$$

Here, $\partial I^e/\partial n$ denotes the outward normal derivative of I^e, constants α^e and γ^e are defined in terms of μ_a^e and κ^e as part of the diffusion approximation and $\mathbf{r}_s$ denotes the source location at the boundary.

Next, we consider that a portion of I^e is absorbed by the fluorophores and re-emitted. The transportation of emitted light I^f is then modeled by

$$\frac{1}{c}\frac{\partial I^f}{\partial t} - \nabla\cdot(\kappa^f \nabla I^f) + \mu_a^f I^f = Q(\mathbf{r}, t) \quad \text{in } \Omega \times (0, T], \quad (4)$$

with κ^f denoting the diffusion coefficient and μ_a^f denoting the absorption coefficient at the exciting wavelength. Here, the emission of fluorescent light is due to the excited interior source [5],

$$Q(\mathbf{r}, t) = \chi(\mathbf{r})h(\mathbf{r}) \int_0^t e^{-(t-t')/\tau(\mathbf{r})} I^e(\mathbf{r}, t')dt', \quad (5)$$

where $\chi(\mathbf{r})$ is the indicator function, $h(\mathbf{r})$ is the fluorophore concentration, and $\tau(\mathbf{r})$ is the fluorescence-lifetime. We solve (4) subject to initial condition

$$I^f(\mathbf{r}, 0) = 0 \quad \text{in } \Omega, \quad (6)$$

and boundary condition

$$I^f + \alpha^f \kappa^f \frac{\partial I^f}{\partial n} = 0 \ \text{ on } \partial\Omega. \quad (7)$$

Upon solution of the initial-boundary value problem for emission light consisisting of (4) subject to (6) and (7), we model measurements of scattered light leaving the boundary of the medium, $u(\mathbf{r}, t)$, through evaluation of

$$u(\mathbf{r}, t) = -\kappa^f \frac{\partial I^f}{\partial n} = \frac{1}{\alpha^f} I^f \quad \text{on } \partial\Omega \times (0, T]. \quad (8)$$

Note that we have substituted (7) into the first result of (8) to obtain the final result of (8).

Suppose we consider the time-averaged data defined as

$$\bar{u}(\mathbf{r}) = \frac{1}{\alpha^f}\bar{I}^f(\mathbf{r}) = \frac{1}{\alpha^f T}\int_0^T I^f(\mathbf{r}, t)\mathrm{d}t \quad \text{on } \partial\Omega. \quad (9)$$

The steady-state optical fluence rate for emission light, $\bar{I}^f$, satisfies the steady-state diffusion equation

$$-\kappa^f \nabla^2 \bar{I}^f + \mu_a \bar{I}^f = \bar{Q} \quad \text{in } \Omega, \quad (10)$$

subject to the boundary condition

$$\bar{I}^f + \alpha^f \kappa^f \partial_n \bar{I}^f = 0 \quad \text{on } \partial\Omega. \quad (11)$$

We will make use of this boundary value problem consisting of (10) subject to (11) in the analysis that follows.

Inverse problem: The measurements of the scattered light leaving the boundary of the medium are taken at M distinct locations denoted by $\mathbf{r}_m \in \partial\Omega$ for $m = 1, \cdots, M$. Moreover, N samples of these measurements in time are collected with sampling rate, Δt with $T = N\Delta t$. The observed collection of data is given by the vector $\mathbf{u} \in \mathbb{R}^{MN}$ with $\mathbf{u} = [u(\mathbf{r}_1, t_1), \cdots, u(\mathbf{r}_M, t_1), u(\mathbf{r}_1, t_2), \cdots, u(\mathbf{r}_M, t_N)]$. Because these measurements have relatively low photon counts, we model the noise in the data using Poisson statistics.

The inverse problem seeks to reconstruct the sparse spatial distribution of fluorescence lifetime appearing in (5) from the set of noisy measurements in $\mathbf{u}$. We assume that the fluorophores are concentrated only in a small area. Furthermore, we assume that the optical properties of the medium for excitation and emission are known, i.e., κ^e, κ^f, μ_a^e, and μ_a^f are known. Therefore, this inverse problem is linear. However, the problem is ill-posed. Hence, we include a regularization term that promotes sparsity in the solution. We propose the following three-stage method for reconstructing the fluorescence sources:

Step 1: Assuming a sparse distribution of fluorescence sources that does not change over $[0, T]$, we apply SPIRAL-ℓ_p [6], a nonconvex, sparsity promoting optimization method, to determine the spatial support, $\chi(\mathbf{r})$ of the sources from the time-averaged data in (9). (We describe the SPIRAL-ℓ_p method in the next section.)

Step 2: Using the determined support $\chi(\mathbf{r})$ of the sources from Step 1, we apply SPIRAL-ℓ_1 [9] to determin $Q(\mathbf{r}, t)$ from the time-dependent measurements. Since we have identified the support in Step 1 and therefore no longer need to promote sparsity in the solution, we use SPIRAL-ℓ_1 with a negligible regularization penalty parameter.

Step 3: Using $\chi(\mathbf{r})$ and $Q(\mathbf{r}, t)$ from Steps 1 and 2, we apply a nonlinear least squares solver to recover the fluorophore concentration $h(\mathbf{r})$ and the lifetime $\tau(\mathbf{r})$ from (5).

Related methods: Previous work for solving Poisson inverse problems include statistical multiscale modeling and analysis frameworks [10], nonparametric estimators using wavelet decompositions [11], and combination expectation-maximization algorithms with a total variation-based regularization [12]. Our proposed approach uses a sequence of separable approximations to the objective function with non-convex p-norm regularization to identify the support of the time-dependent fluorescence sources and to recover their lifetime parameters.

3. METHODOLOGY

Finite difference discretization: Both initial-boundary value problems (1) and (4) subject to the initial and boundary conditions ((2), (3) and (6), (7) respectively) are solved using the Crank-Nicolson method [13]. As defined in (8), in the discrete setting, the measurements are obtained by restricting the numerical solution of emission light, say $\mathbf{V}$, to the boundary:

$$\mathbf{u} = \frac{1}{\alpha^f}\mathbf{R}\mathbf{V} = \frac{1}{\alpha^f}\mathbf{R}\mathbf{L}^{-1}\tilde{\mathbf{Q}}, \quad (12)$$

where $\mathbf{R}$ is a boundary restriction operator, $\mathbf{L}$ is the finite difference operator and $\tilde{\mathbf{Q}}$ is averaged Q between consecutive time steps. More over, $\frac{1}{\alpha^f}\mathbf{R}\mathbf{L}^{-1}$ is defined as the system matrix $\mathbf{A}$ for the inverse algorithm. Instead of generating the system matrix $\mathbf{A}$ explicitly, we compute the action $\mathbf{A}(\mathbf{x})$ and $\mathbf{A}^T(\mathbf{x})$ on-the-fly using the forward and backward substitution techniques. Similarly, actions of the steady-state boundary value problem in (10) and (11) also have to be constructed in a similar technique.

Poisson intensity reconstruction: The arrival of photons at a detector is typically modeled by a Poisson noise model [14], $\mathbf{y} \sim \text{Poisson}(\mathbf{A}\mathbf{f}^*)$, where $\mathbf{y} \in \mathbb{Z}_+^m$ is the vector of observed photon counts, $\mathbf{f}^* \in \mathbb{R}_+^n$ is the vector of true signal intensity, and $\mathbf{A} \in \mathbb{R}_+^{m\times n}$ is the system matrix. The negative Poisson log-likelihood function corresponding to observing $\mathbf{y}$ given $\mathbf{A}\mathbf{f}$ is given by

$$F(\mathbf{f}) = \mathbf{1}^T\mathbf{A}\mathbf{f} - \sum_{i=1}^{m} y_i \ \log(\mathbf{e}_i^T\mathbf{A}\mathbf{f}), \tag{13}$$

where $\mathbf{1}$ is the m-vector of ones and $\mathbf{e}_i$ is the i-th column of the $m \times m$ identity matrix. A small parameter $\epsilon > 0$ is often added within the $\log$ term in (13) to avoid singularity when $\mathbf{f} = 0$ [15].

We formulate our Poisson reconstruction problem as the following constrained optimization problem:

$$\begin{aligned} \hat{\mathbf{f}} \quad = \quad & \underset{f\in\mathbb{R}^n}{\arg\min} \qquad \Phi(\mathbf{f}) \equiv F(\mathbf{f}) + \beta \, \|\mathbf{f}\|_p^p \\ & \text{subject to} \quad\ \mathbf{f} \succeq 0. \end{aligned} \tag{14}$$

where $\|\mathbf{f}\|_p^p$ $(0 \leq p < 1)$ is a penalty function that promotes sparsity in our solution and $\beta > 0$ is a scalar regularization parameter. The nonnegativity constraint on $\mathbf{f}$ ensures that the solution, which corresponds to the fluorescence sources, is nonnegative. Our optimization problem formulation is different from the more commonly used least-squares minimization problem [5] in three ways: (1) instead of a least-squares data-fidelity term, we use a negative log-likelihood function to model the noise statistics more accurately; (2) instead of a Tikhonov regularization or a sparsity-promoting ℓ_1-norm, we use a non-convex p-norm, where $0 \leq p < 1$, to bridge the convex ℓ_1-norm and the ℓ_0 counting semi-norm; and (3) we enforce a nonnegativity constraint on our solution. We solve the minimization problem (14) using the SPIRAL-ℓ_p approach (see [6, 16, 17] for further details).

4. NUMERICAL EXPERIMENTS

In this section, we apply the proposed three-stage reconstruction method for 2D fluorescence lifetime imaging problems. For the MATLAB simulations, we used a unit square domain $\Omega = (0, 1) \times (0, 1)$ with the following non-dimensionalized optical properties: the absorption coefficient $\mu_a = 0.05$ and the diffusion coefficient $\kappa = 0.0476$ [3]. For all experiments, $N = 200$ time-level samples from $M = 72$ boundary detectors with sampling rate $\Delta t = 0.05$ are colloected using 5 exterior near-infrared source points. Also, the fluorescence-lifetime and the fluorophore concentration are set to 5.7 and 2000, respectively [18]. The simulated boundary measurements are corrupted by Poisson noise using the MATLAB's `poissrnd` function. The noise level (%) is computed as $100 \cdot \|\mathbf{A}\mathbf{f}^* - \mathbf{y}\|_2/\|\mathbf{y}\|_2$. The SPIRAL-$\ell_p$ and SPIRAL-ℓ_1 algorithms in stage (1) and (2) are initialized using $\mathbf{A}^T\mathbf{y}$ and terminate if the relative objective values do not significantly change, i.e., $|\Phi(\mathbf{f}^{k+1}) - \Phi(\mathbf{f}^k)|/|\Phi(\mathbf{f}^k)| \leq 10^{-7}$. The regularization parameters (β) for both experiments are manually optimized to get the minimum RMSE (RMSE (%) $=$ $100 \cdot \|\hat{\mathbf{f}} - \mathbf{f}^*\|_2/\|\mathbf{f}^*\|_2$, where $\hat{\mathbf{f}}$ is an estimate of $\mathbf{f}^*$).

In this paper, we consider two experiments. Experiment 1 consists of a fluorescence reconstruction problem with two fluorophore point sources (see Fig. 1(a)) while Experiment 2 consists of two islands of fluorophore sources (see Fig. 5(a)) The observations $\mathbf{u}$ are time dependent and are corrupted by Poisson noise (see e.g., Fig. 2(a)). Step 1 of our proposed method uses the time-averaged measurements $\bar{\mathbf{u}}$ (see e.g., Fig. 2(b)) to obtain an estimate for the support of the fluorophores for all 5 exterior sources (see e.g., Fig. 3). The final reconstructed support of the fluorophores is obtained by thresholding and computing the mode of the SPIRAL-ℓ_p reconstruction since the location of the fluorophores must be the same for each source (see Figs. 1(b) and 5(b)). Then given the estimated support from Step 1, in Step 2 we reconstructed $\tilde{\mathbf{Q}}$ in (12) using SPIRAL-ℓ_1 with negligible regularization since we already identified the support and no longer need to promote sparsity in the solution (see e.g., Fig. 4). In Step 3, we used the built-in Matlab nonlinear least-squares command `lsqnonlin` to compute the estimate $\hat{h}$ at the two source locations using the initial concentration value $\hat{h}_0 = 1.0$ for both locations and initial fluorescence lifetime value $\hat{\tau}_0 = 1.0$. Results are presented in Tables 1 and 2.

5. CONCLUSION

In this paper, we proposed a novel three-stage method to solve the fluorescence lifetime imaging problem from Poisson noise corrupted boundary measurements. For this imaging problem, measured signals are modeled by solutions of a coupled initial-boundary value problem for light scattering and absorption inside the sample. Furthermore, unlike previous methods, Poisson noise is explicitly modeled in the inverse problem and a nonconvex sparse recovery method (SPIRAL-ℓ_p) is used to determine the support of the fluorophores. Numerical experiments for small scale problems demonstrate that the proposed method accurately solves the FLIM problem. Future work will include larger-scale real data studies with different optical properties (i.e., absorption and diffusion coefficients).

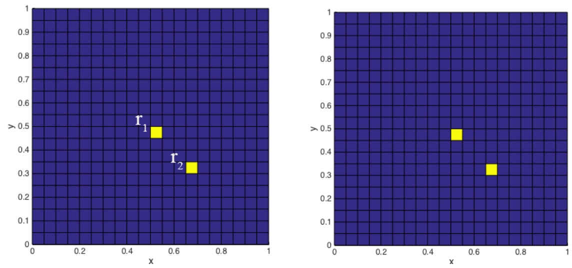

(a) True support (b) Reconstructed support

Fig. 1. True 2D support and our computed reconstruction for Experiment 1: (a) True fluorophore locations in the 2D grid, (b) Final reconstructed support of the fluorophore by thresholding and computing the mode of the results in Fig. 3.

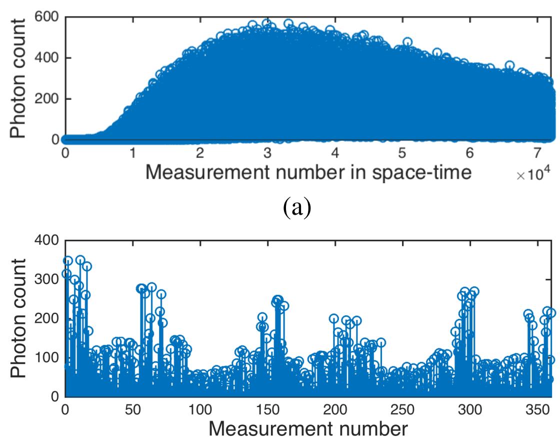

(a)

(b)

Fig. 2. Measurements for Experiment 1: (a) Time-dependent measurements $\mathbf{u}$ corrupted by 7.5% Poisson noise, (b) Time-averaged measurements $\bar{\mathbf{u}}$ at the 360 boundary detectors (72 detectors per one exterior source).

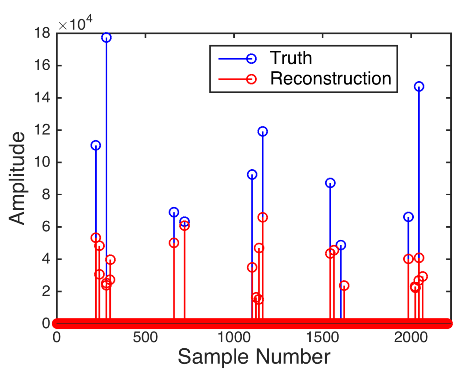

Fig. 3. Support reconstruction for Experiment 1 for all 5 sources using SPIRAL-ℓ_p method ($p = 0.3$) in stage 1 of our proposed method. Here, RMSE = 0.79 and 23 nonzero components are in the reconstruction.

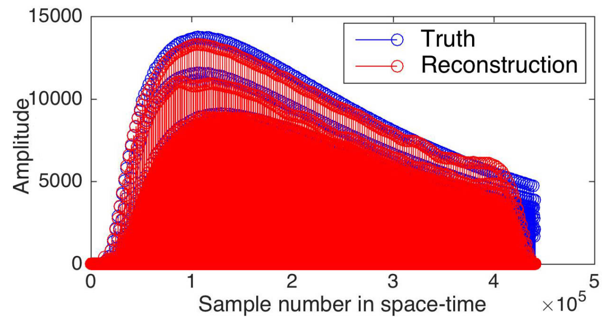

Fig. 4. Experiment 1 SPIRAL-ℓ_1 reconstruction of $\tilde{\mathbf{Q}}$ with the given reconstructed support in Fig. 1(b). RMSE of the reconstruction is 0.108.

	Ground Truth	Estimate
$h(r_1)$	2.00×10^3	2.07×10^3
$h(r_2)$	2.00×10^3	1.95×10^3
τ	5.70	5.64

Table 1. A comparison between the true and the computed fluorophore concentrations, h, at point locations r_1 and r_2 and between the true and computed fluorescence lifetimes, τ for Experiment 1.

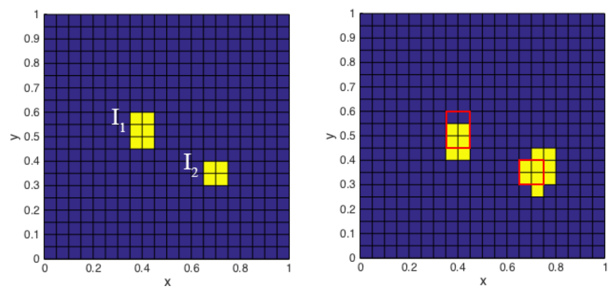

(a) True support (b) Reconstructed support

Fig. 5. Reconstructed 2D support vs. true support of the fluorophore islands for Experiment 2: (a) True fluorophore islands in the 2D grid, (b) Reconstructed support of the fluorophore by thresholding and computing the mode of the SPIRAL-ℓ_p ($p = 0.1$) reconstruction.

	Ground Truth	Range of Estimate
$h(I_1)$	2.00×10^3	1.29×10^3 to 2.72×10^3
$h(I_2)$	2.00×10^3	0.58×10^3 to 0.95×10^3
τ	5.70	5.76

Table 2. A comparison between the true and the computed fluorophore concentrations, h, at islands I_1 and I_2 and between the true and computed fluorescence lifetimes, τ, for Experiment 2.

6. REFERENCES

[1] S. R. Swift and L. Trinkle-Mulcahy, "Basic principles of FRAP, FLIM and FRET," *Proc R Microsc Soc.*, vol. 39, pp. 3–10, 2004.

[2] H. C. Ishikawa-Ankerhold, R. Ankerhold, and G. P. C. Drummen, "Advanced fluorescence microscopy techniques – FRAP, FLIP, FLAP, FRET and FLIM," *Molecules*, vol. 17, no. 4, pp. 4047, 2012.

[3] D. Álvarez, P. Medina, and M. Moscoso, "Fluorescence lifetime imaging from time resolved measurements using a shape-based approach," *Opt. Express*, vol. 17, no. 11, pp. 8843–8855, May 2009.

[4] S. Bloch, F. Lesage, L. McIntosh, A. Gandjbakhche, K. Liang, and S. Achilefu, "Whole-body fluorescence lifetime imaging of a tumor-targeted near-infrared molecular probe in mice," *Journal of Biomedical Optics*, vol. 10, no. 5, pp. 054003–054003–8, 2005.

[5] S. R. Arridge and J. C. Schotland, "Optical tomography: forward and inverse problems," *Inverse Problems*, vol. 25, no. 12, pp. 123010, 2009.

[6] L. Adhikari and R. F. Marcia, "Nonconvex relaxation for poisson intensity reconstruction," in *2015 IEEE International Conference on Acoustics, Speech and Signal Processing (ICASSP)*, April 2015, pp. 1483–1487.

[7] Lihong V Wang and Hsin-i Wu, *Biomedical Optics: Principles and Imaging*, John Wiley & Sons, 2012.

[8] S. R. Arridge, "Optical tomography in medical imaging," *Inverse Problems*, vol. 15, no. 2, pp. R41, 1999.

[9] Z. T. Harmany, R. F. Marcia, and R. M. Willett, "This is SPIRAL-TAP: Sparse Poisson intensity reconstruction algorithms - theory and practice," *IEEE Trans. Image Processing*, vol. 21, no. 3, pp. 1084–1096, 2012.

[10] R. D. Nowak and E. D. Kolaczyk, "A statistical multiscale framework for poisson inverse problems," *IEEE Transactions on Information Theory*, vol. 46, no. 5, pp. 1811–1825, Aug 2000.

[11] A. Antoniadis and J. Bigot, "Poisson inverse problems," *The Annals of Statistics*, pp. 2132–2158, 2006.

[12] A. Sawatzky, C. Brune, T. Kösters, F. Wübbeling, and M. Burger, "EM-TV methods for inverse problems with Poisson noise," in *Level Set and PDE Based Reconstruction Methods in Imaging*, pp. 71–142. Springer, 2013.

[13] R. LeVeque, *Finite Difference Methods for Ordinary and Partial Differential Equations: Steady-State and Time-Dependent Problems*, SIAM, Society for Industrial and Applied Mathematics, classics in applied mathematics edition, 7 2007.

[14] D. L. Snyder and M. I. Miller, "Random point processes in space and time," *Springer-Verlag, New York, NY*, 1991.

[15] J. A Fessler and A. O. Hero, "Penalized maximum-likelihood image reconstruction using space-alternating generalized em algorithms," *IEEE Trans. Image Processing*, vol. 4, no. 10, pp. 1417–1429, 1995.

[16] W. Zuo, D. Meng, L. Zhang, X. Feng, and D. Zhang, "A generalized iterated shrinkage algorithm for non-convex sparse coding," in *2013 IEEE International Conf. on Computer Vision*, Dec 2013, pp. 217–224.

[17] A. Orkusyan, L. Adhikari, J. Valenzuela, and R. F. Marcia, "Analysis of p-norm regularized subproblem minimization for sparse photon-limited image recovery," in *2016 IEEE International Conference on Acoustics, Speech and Signal Processing (ICASSP)*, March 2016.

[18] E. Terpetschnig and D. M. Jameson, "Fluorescence lifetime," *ISS Techinical Note*, 2005.